Sustainable Stimuli-Responsive Wound Dressing made of Green Materials

Master's thesis in Materials Chemistry

ROBERT HUMMERHIELM

DEPARTMENT OF CHEMISTRY and CHEMICAL ENGINEERING

CHALMERS UNIVERSITY OF TECHNOLOGY
Gothenburg, Sweden 2022
www.chalmers.se

Master's thesis 2022

Sustainable Stimuli-Responsive Wound Dressing made of Green Materials

ROBERT HUMMERHIELM

CHALMERS
UNIVERSITY OF TECHNOLOGY

Department of Chemistry and Chemical Engineering
Division of Applied Chemistry
Chalmers University of Technology
Gothenburg, Sweden 2022

Sustainable Stimuli-Responsive Wound Dressing made of Green Materials
ROBERT HUMMERHIELM

Supervisor: Roujin Ghaffari, Department of Chemistry and Chemical Engineering
Examiner: Anette Larsson, Department of Chemistry and Chemical Engineering

Master's Thesis 2022
Department of Chemistry and Chemical Engineering
Division of Applied Chemistry
Chalmers University of Technology
SE-412 96 Gothenburg
Telephone +46 31 772 1000

Typeset in LaTeX
Printed by Chalmers Reproservice
Gothenburg, Sweden 2022

Sustainable Stimuli-Responsive Wound Dressing made of Green Materials
ROBERT HUMMERHIELM
Department of Chemistry and Chemical Engineering
Chalmers University of Technology

Abstract

Non-healing chronic wound are wound that have a naturally high infection risk and produce an excess of exudate. To better treat these wounds, having a wound dressing that can absorb much of the exudate, keep the wound environment moist, and administer antibiotics when the wound is infected would be ideal. Here, a wound dressing that can absorb large amounts of exudate and locally administer drugs as a response to high pH commonly seen in infected wounds was prepared. First a carboxymethyl cellulose (CMC) aerogel scaffold was first prepared, using ethylene glycol diglycidyl ether (EGDE) as a cross-linker. The scaffold was then impregnated via diffusion or injection with naproxen-loaded pH-sensitive lignin nanoparticles (LNPs), synthesized using an anti-solvent method. Scanning electron microscopy (SEM) was used to investigate the morphology of the CMC gel as well as the shape and size of the synthesized unloaded and naproxen-loaded LNPs. The LNPs efficiency as drug-vehicles was investigated by loading the LNPs with naproxen and calculating the loading capacity and encapsulation efficiency of naproxen. Fourier Transform IR was used to investigate the cross-linking of CMC and EGDE and a tea bag test was used investigate the swelling capacity of the CMC gel.

During the synthesis of the CMC gel, several parameters were varied. This resulted in aerogels with different morphologies and properties. Depending on the synthesis parameters, a swelling ratio between 28 and 623 g/g. A high swelling capacity was obtained by adding low concentrations of CMC and EGDE. The lowest swelling capacity was obtained by adding high EGDE concentrations and drying the gel via freeze-drying and oven-drying.

Based on the SEM images of LNPs, unloaded and naproxen-loaded LNPs had a desired spherical shape with an average size of 71.6 and 81 nm, respectively. The size distribution was quite large for both LNPs between 31.5–127 nm for unloaded and 26.5–140 nm. The loading capacity of naproxen was around 10% while the encapsulation efficiency was around 48%.

Based on the SEM images of the impregnated aerogels, no LNPs could be found. Either no LNPs were present in the sample taken or the LNPs have dissolved due to high pH.

Keywords: wound dressings, carboxymethyl cellulose, aerogel, lignin nanoparticles, drug-loading.

Acknowledgements

I would like to thank Roujin Ghaffari and Anette Larsson for their supervision and help during this project. Roujin, a huge thank you for giving me the opportunity to be a part of this thesis project as well as all the help and patience you have given me during the project. Anette, thank you for all the advice and help you have given me to keep moving forward with the project.

I would also like to thank Robin Nilsson and Ratchawit Janewithayapun for helping me with lab work and teaching me how to use some of the instruments used during this project.

Lastly, I would also like to thank my family, friends, and other master's thesis workers for supporting me throughout the project.

Robert Hummerhielm, Gothenburg, June 2022

Contents

List of Figures

1
Introduction

Chronic non-healing wounds, such as burn wounds, diabetic ulcers, and leg ulcers, place a major burden on patients. They cause pain, infections, and loss of function, and if they are not treated correctly, often lead to amputation and sepsis [1]. Chronic non-healing wounds are predominantly found in elders [2], but also affect many people with obesity and diabetes [1]. Due to an aging population and an increasing rate of obesity and diabetes, chronic non-healing wounds have become a silent epidemic and major challenge for the health care system [1–3].

Chronic non-healing wounds have a longer than expected healing time, due to excessive inflammation, and thus need an extended period of care. As a consequence, there is an increased risk of infection [2–4]. Infected wounds have locally elevated pH levels, which results in increased rates of bacterial growth and reduces the rate of healing [5]. Treating the infection is vital as untreated infections can be fatal. Commonly, oral administration of antibiotics is used for treatment; however, due to the systemic effect the effective dosage is low and there is a significant risk of overuse that can lead to bacteria becoming antimicrobial resistant [6]. Consequently, localized drug administration is desirable to better treat infections and promote healing.

Wound dressings are primarily used to protect the wound and hinder bacteria from entering the wound [4, 7, 8]. Standard cotton gauzes are often used; however, they make the wound dry leading to increased pain and discomfort. Thus, more ideal wound dressings, such as hydrogels, foams, and alginate dressings, have been developed that aim to create a better wound environment for healing and patient comfort. These advanced dressings can also act as a drug delivery system for localized drug administration. Although advanced dressings improve upon the traditional dressings, they are costly—especially when drug-loaded. Thus, it is necessary to make them more cost-competitive.

Bio-based materials such as lignin, cellulose, and chitosan are environmentally friendly materials that due to their abundance often are inexpensive. They are also benign to humans as well as biocompatible and biodegradable, making them excellent materials for wound dressings and drug delivery applications. Cellulose is a biopolymer commonly used for wound dressings due to its accessibility and suitable properties such as biocompatibility, non-toxicity, inexpensive, and water absorbance [4, 9].
Lignin is an interesting material for use in biomedical applications as a drug delivery vehicle due to being non-toxic, biocompatible, biodegradable, antimicrobial activity, pH-responsive, and low pro-inflammatory [10, 11]. Lignin nanoparticles (LNPs)

have been shown to be good drug carriers that have a sustained drug release and increase drug efficacy, selectivity, and drug stability [10]. Thus, LNPs would make for an attractive drug delivery system with great properties. When coupled with an appropriate wound dressing, LNPs would provide a stimuli-responsive and effective drug delivery system that can accelerate the healing process of the tissue immensely.

1.1 Aims

The aim of this project is to create a wound dressing impregnated with a pH-responsive drug delivery vehicle that can be used for chronic wounds. Therefore, it is important that the wound dressing is biocompatible and biodegradable, and that the type of wound dressing used is able to absorb exudate and have enough wet stability to not break down during removal. It is also important that the drug delivery vehicle is responsive to increases in pH so that it will release the loaded drug when a wound becomes infected.

1.2 Limitations

While there are many methods of synthesis methods and materials that can potentially be used in the wound dressing, this project will be limited to synthesizing an aerogel, via heat treatment, made of carboxymethyl cellulose (as the matrix material) and ethylene glycol diglycidyl ether (as the crosslinker).

Similarly, lignin nanoparticles can be synthesized and drug-loaded in various ways. Therefore, an anti-solvent method will be used for the synthesis of LNPs, and the drug will be loaded via entrapment. Furthermore, one model drug, naproxen, will be used to examine the efficiency of the LNPs as a drug carrier.

2
Theory

2.1 Wound Healing

A wound can generally be defined as any damage to or loss of tissue, such as a cut or a burn [4, 9]. Wounds can be classified into different categories to better help with understanding the necessary wound treatment and management. The broadest classification is that of acute and chronic wounds, which is based on the repair process of the wound [4, 9, 12]. Acute wounds heal in a timely matter and usually without any complications. Chronic wounds, on the other hand, are more problematic and take a long time to heal, and often reoccur. Since the healing process of wounds is a complex interplay between the different parts of the body to grow and regenerate tissue, disruptions in the process can have a significant negative impact and cause complications. The process can be divided into four phases that always occur in the following order: hemostasis, inflammation, proliferation, and remodeling [2, 4].

The first phase, hemostasis, occurs directly after the injury and is characterized by restricted blood flow and blood clotting. The next phase, inflammation, starts essentially alongside hemostasis and is an immune response to remove and clean up the wound from bacteria, foreign particles, and dead cells. As the inflammatory phase subsides, growth factor is released in the wound and the proliferation phase occurs. Here, the tissue in the wound is starting to be rebuilt and new tissue is formed. The last phase of wound healing is the remodeling phase, where the wound is fully closed, and collagen fibers in the skin are reorganized and strengthened [1, 2, 4]. Since these four phases always occur in order, having underlain physiological problems (such as diabetes) or tissue insults that hinder one phase to conclude and another one to start, will stop the wound from healing. As a result, the healing time is prolonged and can make the wound chronic.

2.2 Chronic Wounds

Chronic wounds are tissue injuries that are slow to heal, take longer than 12 weeks to heal, and often reoccur in patients [1, 4]. The long healing time can be attributed to repeated tissue insults or underlying physiological conditions that keep the wound in an inflammatory state and impede the healing process [1, 4]. The prolonged inflammation causes the wound to produce excess amounts of exudate (wound fluid) which causes healthy tissue around the wound to break down and further impede the wound healing process [4]. It should be stated that exudate itself is an essential

part to wound healing as it keeps the wound environment moist as well as provide the wound with nutrients and cells that help control pathogens. It is only when an excess amount of exudate is present that it becomes corrosive and negatively affects the healing process [4]. A major consequence of the long healing time of chronic wounds is the high infection risk. If bacteria infect the wound and are allowed to grow, they will create a protective biofilm that is difficult to remove via drug treatments. As a result, preventing infections is key to reducing the healing time.

2.3 Wound Dressings

Wound dressings are used to cover wounds and primarily act as a physical barrier to keep the wound clean and free from foreign material, infections, and necrotic tissue (dead tissue) [13, 14]. Ideally, wound dressings should help to improve the healing process; however, it is not necessary as long as the dressing does not impede the healing process by for instance damaging new tissue, adhering to the wound, or leaching toxic compounds.

An ideal wound dressing is regarded as a dressing that effectively promotes the healing process and is cost-effective. Such a wound dressing should ensure optimal healing by [4, 6, 7, 13, 14]:

- maintaining high humidity/moisture,
- remove excess wound exudate,
- allowing thermal insulation,
- allowing gaseous exchange,
- conforming to the wound surface,
- facilitating, when necessary, debridement (*i.e.* removing dead, damaged, or infected tissue),
- minimizing scar formation,
- being impermeable to extraneous bacteria,
- being non-toxic,
- being non-adherent, comfortable, and conforming.

There are many types of wound dressings available for use, some are used in a wide range of cases, and others are more specialized. Traditional wound dressings, such as cotton wool, gauzes, and bandages, are dry dressings that aim to keep the wound dry and warm [4, 14]. They generally work for most types of wounds, but the dry wound environment they cause is unfavorable for the healing process. Furthermore, they risk adhering to the wound, which will cause pain and potential damage to new tissue when removed [4, 14]. To better treat wounds, more advanced wound dressings, such as hydrogels, foams, and hydrocolloids, have been developed. These types of dressings have been developed with different aspects of the wound healing process in mind, to better create a wound environment more suited for healing [14]. Although synthetic polymers, such as polyurethane, are used in wound dressings,

the need for non-toxic, biocompatible. and biodegradable materials make biopolymers much more attractive—hence, the wide use of cellulose, chitin, and alginate in basic and advanced dressings. Nonetheless, since wounds can be very different and the wound environment changes as it heals, advanced wound dressings will never be ideal to use throughout the whole treatment [6, 14]. As such, there is a need for different types of dressings that provide the correct support for specific healing stages and environments to aid and improve the healing process.

Hydrogels are 3D porous polymeric networks that are swollen with water. Due to their high moisture content, hydrogels are excellent at maintaining a moist wound environment, relieving pain, can facilitate autolytic debridement, and having a low adherence to the wound. The high moisture content means that hydrogels generally only absorb small amounts of exudate. Foams are similar to hydrogels; however, they are not hydrated and only consist of a 3D porous polymeric network. Due to the low moisture content, foams are able to absorb much more amounts of exudate, which makes them able to maintain a moist wound environment but is not suitable for dry wounds. It also allows for gas exchange to keep a good moisture balance and can act as a matrix to facilitate cellular growth [4, 6, 7, 14].

2.4 Drug Delivery Systems and Drug Release

To aid wound healing (such as providing growth factors or preventing infections) drugs can be used, and how the drug is delivered to the body or specific area of the body is called a drug delivery system. Conventionally, drug delivery systems have generally been administrated in ways where the therapeutic effect is systemic (*i.e.* affecting the entire body). In many cases, this is unwanted as it limits the effective dose reaching the necessary region(s) and reduces the effectiveness of the treatment [15]. For infected wounds, antimicrobial or antibiotic substances are used, however, unnecessary use will impair the healing processes and lead to the formation of antibiotic-resistant bacteria [6, 15].

One way to increase the effectiveness and reduce the use of antimicrobial/antibiotic substances is to administer them topically (*i.e.* administrated to a specific area on or in the body) to have a local effect instead of systemic [4, 6]. Advanced wound dressings loaded with drugs (also called medicated wound dressings) are used to provide a topical administration as the drug will first and foremost be released in the wound area [4, 6, 14]. Another delivery strategy is to use dressings containing drug delivery carriers, such as nanoparticles, that could improve the stability of the encapsulated drug as well as improve the solubility, absorption, and sustained release [10, 11]. Furthermore, nanoparticles decrease the clearance (*i.e.* how fast the drug is removed from the blood plasma), and thus, increase the efficiency of the treatment [10].

When using drug carriers such as nanoparticles, the drug release must be done in a controlled manner in order to make it beneficial. Drug release is the process of drug

migration from the inside of a carrier to the outside of the carrier [16]. Drug release depends on a number of factors related to the carrier material, the drug, and the release medium, such as drug solubility, pH and temperature of the release medium, and degradation of carrier material [16, 17]. Thus, it is essential to consider the drug, the carrier material, and the application of the drug delivery system.

Based on the drug release from the drug carriers, they can broadly be classified as passive and active drug delivery systems. In passive drug delivery systems, the release of the drug is reliant on diffusion from the drug carrier matrix to the wound. In other words, there is no control over when the drug is released. In contrast, active delivery releases the loaded drug upon environmental stimuli (such as pH and temperature) or external stimuli (such as an applied electric or magnetic field) [6]. Although passive drug release is much more efficient than systemic drug administration methods, it does not account for the dynamic wound environment and the optimal timing for administration. Furthermore, over-administration of drugs could lead to negative effects. Thus, active drug delivery systems are more attractive due to their more controlled on-demand release and efficiency [6].

2.5 Aerogel

An aerogel is a gel that is made up of a 3D porous network where the liquid phase has been replaced with gas [18, 19]. Due to being highly porous materials (between 80–99.9%), aerogels have a large surface area and low density which make them promising for a number of uses such as insulation and biomedical applications [18]. Commonly, aerogels are made from silica, however, due to the poor mechanical properties and high production costs, other materials have become more common over the years. Although new materials are used, the methods of production are still based on wet chemistry [18, 20]. As a consequence, the gels must be dried in order to become aerogels. However, based on the drying method, the dried gel will not always be referred to as an aerogel. If the material is freeze-dried, supercritical dried, or dried in an oven or ambient conditions, it is referred to as a cryogel, an aerogel, or xerogel, respectively [18, 21]. Here, aerogel will be used for all three regardless of the drying method used. Especially so since cryogel also refers to hydrogels made in cryogenic temperatures.

2.5.1 Synthesis of Aerogels

The general procedure to synthesize an aerogel is through a sol-gel process where a gel is first formed and then dried to obtain an aerogel [18, 20]. However, the steps involved will vary depending on the precursor used (inorganic, organic, or a combination of both) [21]. In the case of using biopolymers as the precursor, the polymer is dissolved in a solution to form colloidal suspension (sol). Upon dissolution, the polymer will naturally start to rearrange into a porous network and form a gel [22]. The formation of a gel can be determined using either a tilting method or rheological measurements [18]. In the former, a gel has formed if the content does not flow when the container is tilted 70 ° or inverted. In the latter, a gel has formed

when the storage modulus is equal to the loss modulus.

Some polymers, such as cellulose, will form a gel by forming physical crosslinks (*i.e.* physical interactions such as van der Waals forces, chain entanglement, and hydrogen bonds) between chains. Other polymers, such as carboxymethyl cellulose, cannot form a gel through physical crosslinking [22]. Instead, the polymer chains are crosslinked chemically by adding a bi- or multifunctional crosslinking agent that covalently binds two chains together [18, 20–22]. Although chemical crosslinking is normally done at elevated temperatures due to rapid crosslinking, it can also be done at cryogenic temperatures (temperatures below the freezing temperature of the solvent). This is sometimes argued to be a better method due to the lower concentration of crosslinker required and better mechanical properties [23–25]; nonetheless, the reaction time is much slower [25].

As a hydrogel is synthesized via the sol-gel method, the liquid (usually water) in the gel must be removed in order to become an aerogel. There are several drying methods available, but the most common ones are freeze-drying and supercritical drying [18, 21]. Freeze-drying and supercritical drying better preserve the structure of the gel compared to drying the gel under ambient conditions due to the much smaller capillary forces [18, 21]. Although supercritical drying is commonly used, it can be a cumbersome process and requires the water to be solvent exchanged (which makes it less green). Freeze-drying is a simple method of drying materials where the material is fully frozen before the water (ice) is removed via sublimation in a vacuum. The freezing process of the hydrogels will affect the final properties of the resulting aerogel as it determines the pore size. Freezing the hydrogel at around -20°C results in an aerogel with larger pores and a wider pore size distribution due to larger ice crystals forming owning to a low nucleation rate and few nucleation sites. As the freezing temperature decreases, the pores become smaller and more interconnected [18, 21, 24].

2.5.2 Crosslinkers

There is a wide variety of crosslinking agents available; however, few are commonly used for creating biomedical products due to the prerequisite of crosslinkers having to be non-toxic. Some common crosslinkers such as ethylene glycol diglycidyl ether (EGDE), poly(ethylene glycol) diglycidyl ether (PEGDE), divinyl sulfonate (DVS), and glutaraldehyde (GTA) have been shown to have cytocompatibility (*i.e.* non-toxic for cells) and have previously been used as a crosslinker for different biopolymers [25]. Nevertheless, there are still concerns that unreacted species of crosslinker are potentially cytotoxic and if not properly removed can be harmful [26].

EGDE is a bi-functional compound with two epoxide functional groups located at both ends of the molecule. Due to the reactivity of the epoxide groups with hydroxyl, carboxyl, amino, and sulfhydryl groups as well as its non-toxicity/low cytotoxicity and water solubility, it has been used as a crosslinker for many biopolymers (such as DNA, cellulose, and chitosan) [22, 27]. In order to crosslink EGDE and cellulose, the

reaction environment must be strongly alkaline for the hydroxyl groups to become deprotonated and act as nucleophiles. The nucleophilic groups will simultaneously ring-open the epoxide groups and form a covalent bond [22].

2.6 Carboxymethyl Cellulose

Cellulose is one of the most abundant biopolymers and along with it being renewable and inexpensive, makes it an attractive replacement for synthetic fossil-based polymers. Cellulose is a linear polymer that consists of a long chain of connected β-(1,4)-linked D-glucose units [18].

Cellulose has poor water solubility due to the many inter- and intramolecular hydrogen bonds. Therefore, derivatives of cellulose are often used instead as they have similar properties to cellulose, but some of the hydroxyl groups are substituted with other functional groups to enhance solubility in water and non-polar solvents [9, 22].

Carboxymethyl cellulose is a cellulose derivative that has an enhanced water solubility due to the substitution of hydroxyl groups with carboxymethyl groups (CH_2COOH) [22]. CMC retains the same attractive properties as cellulose—namely biocompatibility, biodegradability, non-toxicity, and inexpensiveness—while becoming water-soluble as well as having a higher swelling capacity (due to the carboxylic group becoming negatively charged when dissolved) have made it an attractive material for wound dressings due to its [9]. Wound dressings made from CMC have been shown to be flexible, absorbing exudate, as well as promoting the formation of new blood vessels and autolytic debridement [9].

Although CMC and EGDE have been widely used to make hydrogels, the combination of both has been uncommon. Kundu *et al.* used CMC, xylan, and a combination of both to make hydrogels crosslinked with EGDE via heat treatment. CMC hydrogels were found to have a high swelling capacity in deionized water [28]. Jeong *et al.* used CMC, polyacrylamide, and a combination of both to make hydrogels crosslinked with EGDE or other crosslinkers via heat treatment. CMC hydrogels were found to have a high swelling ratio in deionized water and were shown to have low cytotoxicity [29].

2.7 Lignin

Lignin is the most abundant aromatic biopolymer and can be found in plants between the cell walls of the fibers. Lignin is a polyphenolic polymer that is built from three monolignols syringyl, guaiacyl, and p-hydroxyphenyl that are covalently linked [11, 30, 31]. Although these three building blocks are always present, the amount of each in the composition is different depending on the source material. Furthermore, the extraction method will also affect the final lignin structure and its properties [11, 30, 31].

Considering its origin, lignin is an inexpensive material that is classified as an environmentally friendly material with properties such as biocompatible, biodegradable, and non-toxicity [30–32]. Moreover, it also has properties such as an antimicrobial and anti-inflammatory activity that make it a suitable material for biomedical applications (*e.g.* wound dressing and drug carrier) [10, 11, 33].

2.8 Lignin Nanoparticles

LNPs have gathered much attention in the last decade due to their inexpensiveness, accessibility, renewability, as well as its chemical and physical properties [10, 32, 33]. Studies have shown that LNPs are good carriers for hydrophobic molecules [10, 32, 33], and as such, one of the main applications of LNPs is as a carrier for the delivery of drugs, pesticides, enzymes, and more. Nonetheless, LNPs have also been applied in other fields such as adhesives, nanocomposites, and emulsifiers [11].

In drug delivery, LNPs are used as a drug carrier for many different drugs and other substances used in biomedicine. Figueiredo *et al.* synthesized LNPs loaded with the anti-cancer drugs sorafenib and benzazulene via a solvent-shifting. The resulting LNPs had a controlled and sustained release of the drugs in physiological pH with a high encapsulation efficiency (68% and 77% respectively) but a low loading capacity (7% and 8% respectively) [33]. Alqahtani *et al.* synthesized LNPs loaded with the model drug curcumin (for use in oral administration) via a phase separation method. The LNPs had a high encapsulation efficiency of 92% (no loading capacity was reported) and high stability at low pH and had a controlled and sustained release in physiological pH [10]. Li *et al.* synthesized quaternized LNP-surfactant complex micelles to entrap the anti-inflammatory drug ibuprofen via an anti-solvent method. The LNP micelles had a high encapsulation efficiency of 74% and a high loading capacity of 46%. The LNP micelles were also shown to be stable at low pH and had controlled and sustained release at physiological pH [34].

Although LNPs have advantageous properties for being used as a drug carrier, they must also be efficient. Their efficiency depends on the loading capacity and encapsulation efficiency of the material, in other words, how much drug can be loaded into the material and how efficient the loading is. A review of drug-loaded LNPs made by Sipponen *et al.* shows that LNPs in general have a low loading capacity but a high encapsulation efficiency [32]. Although this makes LNPs, not ideal carriers, they are still suitable for use as a drug carrier [11].

2.8.1 Lignin Nanoparticle Synthesis

LNPs can be synthesized via many different methods which can be divided into chemical, physical, and biological approaches [31]. Some of the most common methods are anti-solvent precipitation, solvent-shifting, polymerization/crosslinking, and ultrasonication [31, 32]. The formation of LNPs is credited to the amphiphilic nature of lignin, regardless of the synthesis method used [31]. Basically, when lignin is dissolved in an organic solvent and then added into water or vice-versa, the hy-

drophobic part of lignin can self-assemble due to hydrophobic interactions. Due to unfavorable interactions with water, the surface area is minimized, and particles are often formed [31]. As a result of the hydrophobic parts of lignin assembling in the core of the nanoparticles, LNPs are a good choice for carrying hydrophobic drugs, but not for hydrophilic drugs.

The most common methods are anti-solvent precipitation and solvent-shifting, which both utilizes an anti-solvent to lower the solubility of lignin and cause them to form nanoparticles [31, 32, 35]. In anti-solvent precipitation, the anti-solvent (usually water) is added to a lignin solution or vice versa. In solvent-shifting, the lignin solution is added to a dialysis bag and then placed in the anti-solvent (usually water). The advantage of using these two methods is the well-defined morphology, shape, and size. Nonetheless, the high solvent consumption especially in anti-precipitation is a drawback [11, 31].

Ultrasonication, on the other hand, is a physical method where the lignin is placed in water and sonicated. The nanoparticles are formed by breaking the lignin into smaller particles. The main advantage of ultrasonication is its use of only water as a solvent, making it a very green method. However, the morphology, shape, and size are non-uniform and are highly dependent on process conditions [11, 31].

2.9 Methods for Drug Loading

There are three main methods of drug-loading nanoparticles: 1) entrapment, 2) encapsulation, and 3) post-loading [17, 32, 36]. The method used is dependent on the drug, the desired release mechanism, and the synthesis conditions for the nanoparticle.

Entrapment is a method where the drug is added before the nanoparticles are formed. When the nanoparticles form, the drug is entrapped in the nanoparticle matrix. The particles could be coated with a different material, depending on the application, to achieve a more controlled drug release [32]. The drug will be released via diffusion through the nanoparticle matrix; however, it could also be released via dissolution of the nanoparticle matrix [17, 32].

Encapsulation is similar to entrapment however there are distinct differences. Here, the drug is encapsulated by the nanoparticle matrix instead of being entrapped within the nanoparticle matrix. Encapsulation can be done in two ways: 1) the drug is dissolved in an emulsion (for example an oil-in-water emulsion) where the oil droplets are encapsulated by lignin, or 2) the drug enters, for example, particles with an oil core encapsulated by a nanoparticle m shell via diffusion [32]. Similar to drugs entrapped in nanoparticles, the drug release will mainly be released via diffusion through the nanoparticle matrix; however, the drug could also be released via shell rupture [32].

Post-loading is a method where the drug is loaded after nanoparticle formation via

different mechanisms depending on the drug used, such as adsorption, electrostatic interactions, and hydrophobic forces [32, 36]. Moreover, post-loading can utilize layer-by-layer adsorption to increase the loading capacity by adsorbing multiple layers of drugs [32]. Nonetheless, due to the drug being adsorbed or surface-bound, the drug is released via desorption, which is more sensitive and not as reliable as encapsulation and entrapment [32].

3
Materials and Methods

3.1 Materials

Carboxymethyl cellulose (M_W = 395 kDa and 725 kDa with a degree of substitution of 0.7) was obtained from Ashland. Ethylene Glycol Diglycidyl Ether was bought from TCI. Softwood Kraft lignin, extracted through LignoBoost^{TM} technology, was provided by a Nordic pulp mill.T.. Naproxen and NaOH were obtained from Sigma-Aldrich. Acetone was obtained from Fisher Scientific. All chemicals were used as received.

3.2 Preparation of Crosslinked CMC Aerogel

In the preparation of the CMC hydrogels, the ratio between CMC and EGDE as well as the concentration of the NaOH solution was changed. A typical procedure was performed as follows: First, 0.2 g of CMC was completely dissolved in 5 mL of 0.1 M aqueous NaOH solution while continuously stirred for 16 h. Subsequently, 338 µL of EGDE was added dropwise to the solution and stirred for 1 h at room temperature. After 1 h, the crosslinking reaction was performed in a water bath at 60 °C for 24 h. The gel was then placed in a 3.5 kDa dialysis bag and dialyzed for 24 h in DI water until the pH of the gel was around 7. Subsequently, the gel was then frozen, with either liquid nitrogen or in a freezer, before being freeze-dried. An overview of the aerogel synthesis procedure can be seen in Figure 3.1.

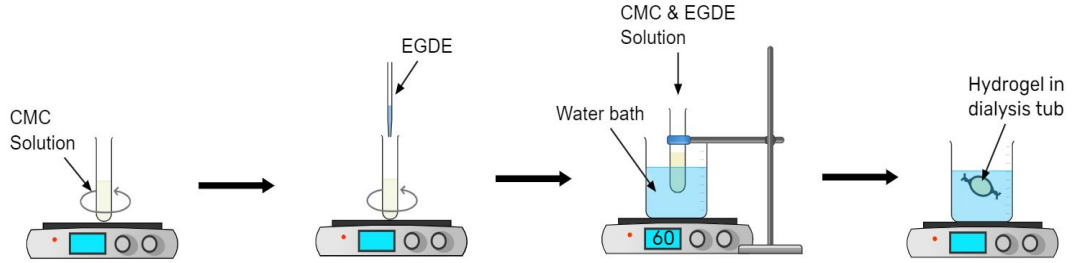

Figure 3.1: A schematic overview of the preparation procedure for the hydrogel before freeze-drying.

3.3 Synthesis and Drug-Loading of LNPs

LNPs were synthesized and drug-loaded via an anti-solvent precipitation method. The overall procedure for synthesis and drug-loading of LNPs is similar, the only difference being the addition of an extra step when loading a drug.

3.3.1 LNP Synthesis

First, 200 mg of lignin was dissolved in 4 g of DI water, followed by adding 12 g of acetone to the solution. This ratio between DI water and acetone was chosen as it is the maximum solubility ratio. The container was covered with parafilm (to avoid evaporation of acetone in the solution) and then stirred with a magnetic stirrer for 3 h at room temperature. Afterward, the solution was filtered twice through a high porosity filter paper (pore size 25 µm) in order to remove any large lignin aggregates. The filtrate was then moved to a new beaker and stirred at high speed while avoiding splashing before 48 mL of DI water (the anti-solvent) was added. The solution was then stirred at 500 rpm for 10 minutes before letting any residual acetone evaporate in a rotary evaporator for 20 min (100 rpm and 20 °C). One last filtration was done with a high porosity filter paper (pore size 25 µm) before measuring the final volume of the solution. The LNP solution was stored in a fridge at 5 °C. An overview of the synthesis process can be seen in Figure 3.2.

The yield of the synthesized LNPs was determined by oven-dry 5 mL of solution and then weighing the dried sample. The mass and volume of the sample were then used to calculate the total mass of LNPs in the solution.

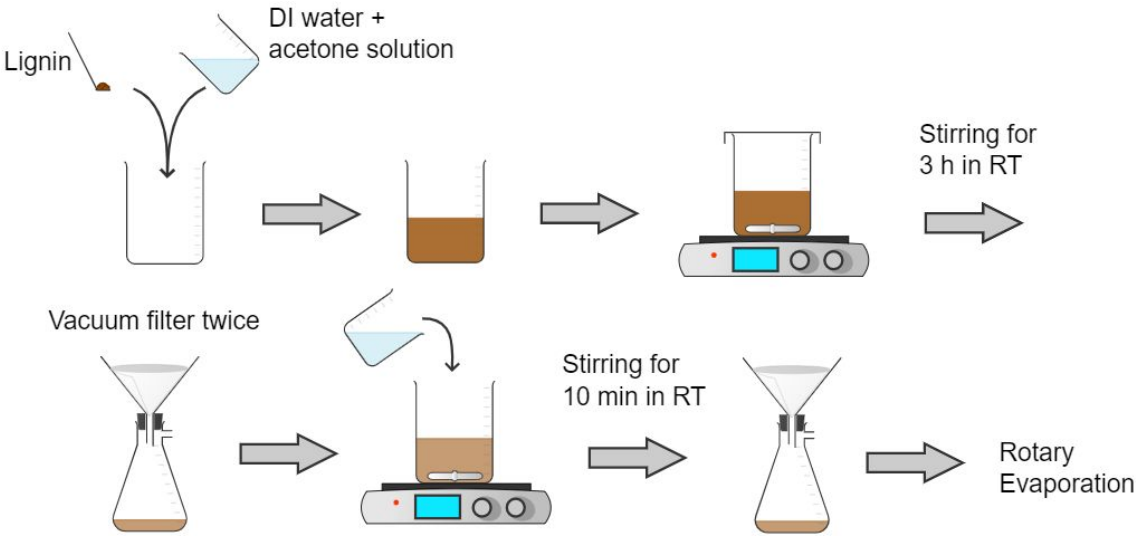

Figure 3.2: A schematic overview of the preparation procedure for the LNPs.

3.3.2 Synthesis of Drug-Loaded LNPs

To synthesize drug-loaded LNPs, a similar procedure to the synthesis of LNPs was done. Naproxen was dissolved in the acetone prior to mixing the acetone with the

lignin-water solution. The ratio between drug and lignin used was 1:10, in other words, 20 mg of drug and 200 mg of lignin was added (following the procedure in Section 3.3.1).

3.4 Impregnation of Aerogels and Hydrogels with LNPs

To impregnate aerogels (dry state) or hydrogels (wet state) with unloaded LNPs or drug-loaded LNPs, the gels were either immersed in 5 mL LNP solution or injected with 1 mL of LNP solution with the help of a thin needle (d = 1.2 mm). 2.5 mL of hydrogel were placed in a syringe (d = 10 mm) and then either kept in a wet state or freeze-dried to a dry state. The sample was then freeze-dried once more for further analysis.

3.5 Characterization

3.5.1 FTIR-ATR Spectroscopy

Spectra of aerogels were collected to analyze the crosslinking of CMC by EGDE using an attenuated total reflectance (ATR) module for a Fourier transform infrared (FTIR) spectrometer (PerkinElmer Frontier FTIR). The resolution of each spectrum was 4 cm^{-1}, and 16 interferograms were taken between 500 and 4000 cm^{-1}.

3.5.2 Morphological Determination

To analyze the morphology of the synthesized aerogels and impregnated aerogels as well as the particle size of unloaded LNPs and drug-loaded LNPs, a SEM (JEOL JSM-7800F Prime) was used. The SEM images were taken at various magnifications with an acceleration potential of 5 kV. Before the measurements, the samples were sputter-coated with gold for 20 seconds (4 nm layer).

3.5.3 Swelling Capacity

The swelling capacity of the synthesized aerogels was characterized via the tea-bag method. Three replicates of each sample were cut, weighed, and then placed in a steel mesh cage. The cage was placed in DI water for 24 h at room temperature. Afterward, the cage was placed on a paper towel and then placed on a paper towel for 2 minutes. After 2 min, the cage was gently wiped with a paper towel to remove free or loosely bound water and the weighed. After removing the aerogel from the steel mesh cage, the same procedure was done with the empty cage to get the wet mass of the cage. The swelling capacity after 24 h was calculated using the following equation:

$$\text{Swelling capacity} = (W_2 - W_1 - W_0)/W_0, \tag{3.1}$$

where W_0 is the mass of the dry sample, W_1 is the mass of the wet steel mesh cage, and W_2 is the mass of wet gel and steel mesh cage.

3.5.4 Loading Capacity and Encapsulation Efficiency

Loading capacity and encapsulation efficiency are the primary indicators to quantitatively determine the LNPs' ability to carry drugs, which can be calculated using equation 3.2 and 3.3. Both equations require the mass of the drug encapsulated in the LNPs to be known. This can either be determined by measuring the concentration of the loaded drug encapsulated and using that to calculate the mass or by measuring the concentration of the non-encapsulated drug and using that to calculate the mass of the drug encapsulated (see equation 3.4). Here, the latter was used to calculate the mass of the drug in the LNPs, *i.e.* the concentration of non-encapsulated drug was measured using a UV-Vis spectrophotometer (Agilent Technologies, Cary 60 UV-Vis).

First, 5 mL of a drug-loaded LNP solution was centrifuged at 9000 rpm for 40 minutes until the supernatant was clear. Afterward, a 1 mL aliquot was taken from the beaker. The aliquot was then diluted, and the drug concentration was analyzed with UV-Vis (at 330 nm for naproxen). The drug concentration in the aliquot was determined with the help of a previously constructed standard curve with known concentrations of naproxen. The concentration of the drug in the aliquot is then used to calculate the total non-encapsulated drug in the solution using equation 3.4. The naproxen standard curve was linear in the concentration range of 0.0015–0.015 mg/mL.

The loading capacity and encapsulation efficiency were then calculated as follows:

$$\text{Loading capacity (\%)} = \left(\frac{\text{mass of drug in LNPs}}{\text{mass of LNPs}}\right) \times 100 \tag{3.2}$$

$$\text{Encapsulation Efficiency (\%)} = \left(\frac{\text{mass of drug in LNPs}}{\text{mass of initially added drug}}\right) \times 100 \tag{3.3}$$

To determine the mass of the drug loaded in the LNPs, the following equation was used:

$$m_{drug,LNPs} = m_{drug,initial} - m_{drug,outside} = m_{drug,initial} - c_{drug,sol} * V_{synthesis}, \tag{3.4}$$

where $m_{drug,LNPs}$ is the mass of loaded drug in the LNPs, $m_{drug,initial}$ is the mass of initially added drug, $m_{drug,outside}$ is the mass of the non-encapsulated drug in the solution, which can be described using the concentration of drug in the solution $c_{drug,sol}$ and the volume of the solution after synthesis $V_{synthesis}$.

4
Results and Discussion

4.1 Preparation of Aerogel

During the preparation of the aerogels different experimental parameters were examined (see Table 4.1). To be able to compare the effect of each parameter, only one parameter was changed at a time. These parameters were chosen as they have been described in the literature to affect the gel formation as well as the properties of the aerogel. There are other factors that also affect the aerogel synthesis such as synthesis temperature and drying method, but due to time constraints, they were not investigated.

To determine the effect of the different parameters, all of the synthesized gels were examined using a tilting method where the reaction container was inverted, and it was observed whether or not the content started to flow. Although this is a quick and simple method to use, it is a qualitative method and thus small differences are difficult to observe.

Table 4.1: A summary of the reaction parameters changed during the gel synthesis and the range in which they were changed.

Parameters varied	Range
NaOH conc.	0.001–1 M
CMC conc.	2.2–3.6 wt.%
EGDE conc.	3.5–12.7 wt.%
CMC M_W	395 & 725 kDa
Freezing temp.	-18 & -196 °C

4.1.1 Effect of NaOH Concentration

During the synthesis, the NaOH concentration was varied between 0.001–1 M. When the containers were inverted, gels made with a NaOH concentration below 0.1 M started to flow and were more similar to a viscous liquid than a gel. Gels made with a NaOH concentration at or above 0.1 M did not flow when inverted and it was determined that a gel had formed. However, there was no noticeable difference in the formed gels when increasing the NaOH concentration from 0.1 M to 1 M. This can possibly be explained by the reaction mechanism of crosslinking EGDE and CMC. As is mentioned in Section 2.5.2, in order to crosslink CMC chains and EGDE, the two epoxide groups on EGDE will be ring-opened by strong nucleophiles.

At high pH ($\geq$ pH 13), the OH-groups on the CMC will readily deprotonate and become highly nucleophilic, thus, enabling crosslinking to occur. It is likely that concentrations of NaOH lower than 0.1 M do not sufficiently deprotonate CMC and that the free OH^- ions in the solution compete with the deprotonated hydroxyl groups on the CMC to ring-open the epoxide groups.

4.1.2 Effect of Crosslinker, Polymer Concentration, and Polymer Molecular Weight

During the synthesis, the EGDE concentration, CMC concentration, and the CMC molecular weight was varied according to Table 4.1. From the tilting test, it was observed that the concentration of EGDE and CMC as well as the CMC molecular weight had a large impact on the gel formation. At low crosslinker concentrations (below 4 wt%), almost all samples would not start flowing when inverted. One sample did start to flow, however, the CMC concentration was a bit lower, which could explain why it did not form a gel. Nonetheless, the formed gels were weak and behaved more like a slime after washing. Increasing the crosslinker concentration resulted in firmer gels and around 7 wt.% the gels could hold a cylindrical shape after removing them from the reaction container. Nonetheless, the gels would not hold a cylindrical shape after washing. Increasing the crosslinker concentration further, to around 13 wt.% resulted in an even firmer gel that would keep its cylindrical shape even after washing.

Varying the CMC concentration had a similar effect on the gel formation as varying the EGDE concentration. Overall, it determined the viscosity of the solution and had a large effect on the firmness of the produced gel. The lower the CMC concentrations were the easier it was to stir the solution, however, the gels synthesized were less firm (*i.e.* behaved more like slime than gels). This is expected as dissolving more CMC would increase the chain entanglements (and other intermolecular interactions) and restrict the movement of the chains, resulting in higher viscosity and firmer gels. Furthermore, the viscosity is also dependent on the molecular weight of the polymer. CMC grades of lower molecular weight will have a lower viscosity when dissolved in water than grades of higher molecular weight. This was observed when changing the CMC from a high molecular weight grade (725 kDa) to a lower one (395 kDa). When around 2.5 wt.% of the 735 kDa grade was dissolved, the solution could not be stirred with a magnetic stirrer (at 1500 rpm at room temperature) after a while. For the 395 kDa grade, this happened when around 4.5 wt.% CMC was dissolved.

The firmest gels, that could keep their shape after washing, were produced when adding 2.2 wt.% 725 kDa CMC and 12.7 wt.% EGDE or 3.5 wt.% 395 kDa CMC and 7 wt.% EGDE.

4.1.3 Effect of Freezing Temperature

As the aerogels were prepared via freeze-drying, the freezing temperature will affect the properties of the aerogels. Freezing hydrogels at -18 °C resulted in overall larger ice crystals forming, which caused the aerogel to have larger holes at the surface after freeze-drying (see Figure A.1 and Figure A.2). Some gels had needle-like ice crystals; however, most did not have them. In contrast, freezing the hydrogels with liquid nitrogen (*i.e.* at -196 °C) resulted in much smaller ice crystals forming, and a more solid aerogel surface was obtained after freeze-drying (see Figure A.3 and Figure A.4). Due to problems with freeze-drying, some of the ice crystals at the surface most likely melted causing a more "popcorn-like" appearance. This is possible as water has strong capillary forces (as was mentioned in Section 2.5.1), which during evaporation would cause damage to the pore structure, especially to aerogels frozen at -196 °C that has weaker pore walls.

As was mentioned in Section 2.5.1, this behavior is expected as the nucleation rate of ice crystals is lower than the growth rate at higher temperatures. When the temperature decreases the nucleation rate increases and new ice crystals form quicker than they grow, causing smaller pores. A consequence of forming many small pores is that the thickness of the gel walls becomes thinner—resulting in lower mechanical strength.

4.2 Swelling Capacity

The swelling capacity of the synthesized aerogels was measured using the tea-bag method (as was mentioned in Section 3.5.3). It is worthwhile to note that due to problems during the freeze-drying some gels were also oven-dried, making it difficult to do a thorough analysis of how each factor affects the swelling capacity. Gels between 3-4 wt.% CMC as well as the 7 wt.% and 13 wt.% EGDE (0.1 M NaOH) did not fully dry and were oven-dried overnight at 50 °C, which resulted in hard and brittle aerogels. Gels that became wrinkly were frozen using liquid nitrogen and had either a hole in the middle or cracks on the edges. This could be due to a weak pore structure that collapsed during freeze-drying, or they started to melt right before or at the start of the freeze-drying process.

As can be seen in Figure 4.1, the aerogel with the highest swelling capacity is the 4.5 wt.% EGDE aerogel with 623 g/g water absorbed. The 7 wt.% EGDE, 2.2 wt.% CMC, 0.1 M aerogel had the lowest swelling capacity only absorbing 28 g/g of water. By comparing Figures 4.1A and 4.1B, a notable trend can be seen where samples that were oven-dried have a much lower swelling capacity compared to only freeze-dried aerogels. This is likely due to the collapsed pore structure of the aerogels that also were oven-dried. Oven-drying or air-drying hydrogel has been shown to destroy the pore structure due to the high capillary pressure acting on the pore walls during water evaporation, causing shrinkage and agglomeration of the pores (*i.e.* bigger pores and decreased porosity) [37]. As mentioned in Section 2.5.1, freeze-drying will, on the other hand, result in a retained pore structure due to the much lower

capillary forces of sublimation compared to evaporation.

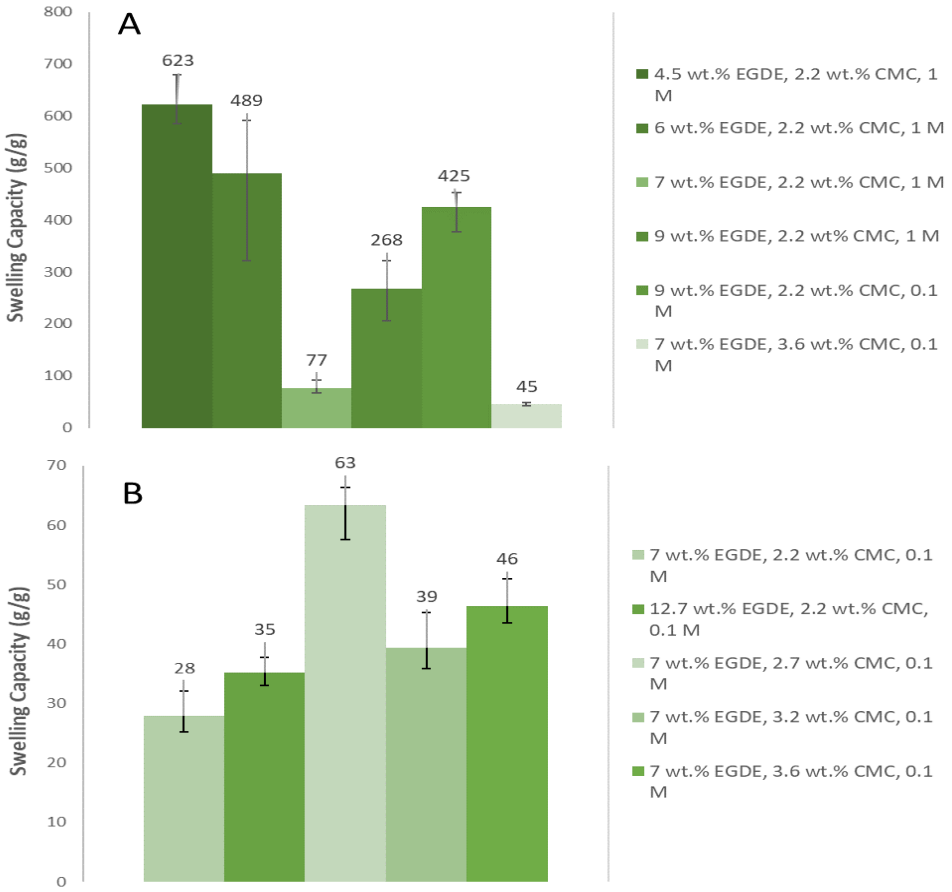

Figure 4.1: The swelling capacity of the hydrogels after being immersed in deionized water for 24 h. Gels that only were freeze-dried are presented in A, while the gels that were freeze-dried and oven-dried are presented in B.

Besides the drying method, there is also a clear difference in swelling capacity between samples with high and low concentrations of crosslinker. The higher the concentration, the lower the swelling capacity. Increasing the crosslinker concentration results in a higher degree of crosslinking. Because of the higher amount of crosslinker present, there is a higher possibility for an EGDE molecule to find and crosslink with deprotonated hydroxyl groups. A higher degree of crosslinking will also result in lower pore size.

The ability to swell is correlated with the following equitation [25]:

$$\pi = \pi_{mix} + \pi_{ion} + \pi_{elastic} \tag{4.1}$$

where π_{mix} is the osmotic pressure from mixing the polymer chains with a solvent, π_{ion} is the osmotic pressure from counter-ions within the gel, and $\pi_{elastic}$ is the opposing elastic pressure from the deformation of the polymer network during swelling. This means that increasing the degree of crosslinking results in higher opposing

elastic pressure from the CMC network during swelling and thus a lower swelling capacity.

Another trend that can be seen is that a higher concentration of CMC leads to lower swelling. A higher concentration of polymer leads to smaller pore size and lower swelling [22]. Furthermore, as the polymer concentration increases the pore walls will become thicker and stronger, which increases the elastic opposing pressure of the CMC network. This further decreases the swelling capacity.

There also seems to be a trend concerning the NaOH concentration used during synthesis. Higher concentration of OH^- would lead to more deprotonation of the OH-groups on the cellulose chains. Thus, there are more possibilities for crosslinking as there are more nucleophilic sites that can perform ring-opening on EGDE and covalently bind with it. As stated before, a higher degree of crosslinking results in a decreased swelling capacity.

4.2.1 Observations of structural stability of swollen aerogels

After swelling for 24 h, the wet aerogels were compressed with a spoon to give an indication of their deformation behavior. The mechanical properties are important, especially of the material in a wet state, as it is undesirable for a wound dressing to break down and enter the wound either during use or removal, which would require the wound to be cleaned up, causing potential tissue damage and unnecessary pain for the patient. However, as was mentioned in Section 2.2 and 2.3, swelling capacity and wet stability are both important factors to consider. They are in opposition with each other as a high swelling capacity leads to low wet stability due to water making the cellulose chains more flexible and less rigid. Having a high swelling capacity is necessary for wound dressings aimed at non-healing chronic wounds, due to the increased time of usage as well as the need to remove excess exudate and control the moisture level of wounds. Thus, it is important to have good stability while maximizing the swelling capacity.

The overall trend that was observed was that the higher the swelling capacity of a sample is, the lower the stability of the aerogel becomes. In the samples with a swelling capacity over 100 g/g, the stability was too low for the gel to keep its structure even when a small amount of force was applied. On the other hand, all of the produced aerogels with a swelling capacity below 100 g/g displayed a much higher wet stability and could withstand compression without separating. The 3.6 wt.% CMC aerogels and the 12.7 wt.% EGDE aerogels were the only aerogels that would display an elastic deformation upon compression (*i.e.* the aerogels would flatten under compression but return to their original shape after removing the force). During compression, water would be released, but most of it would be reabsorbed when the force was released. This indicates that water is not only absorbed by the CMC in the pore walls, but also in the pores themselves. The other aerogels with a swelling capacity below 100 g/g would flatten out upon compression but stay flat

after removing the force (*i.e.* plastically deform).

From these observations and the results of the swelling capacity, it was decided that the aerogel with a composition of 7 wt.% EGDE, 3.6 wt% CMC, and 0.1 M NaOH would be used for impregnation of LNPs, due to the high wet stability, high swelling capacity, and the fact that using fewer crosslinker results in a less expensive wound dressing.

4.3 Chemical Structure of EGDE crosslinked CMC Aerogels

The chemical structure of the EGDE crosslinked CMC aerogels were analyzed using ATR-FTIR. Figure reffig:FTIR represents the spectrum of native CMC and EGDE crosslinked CMC.

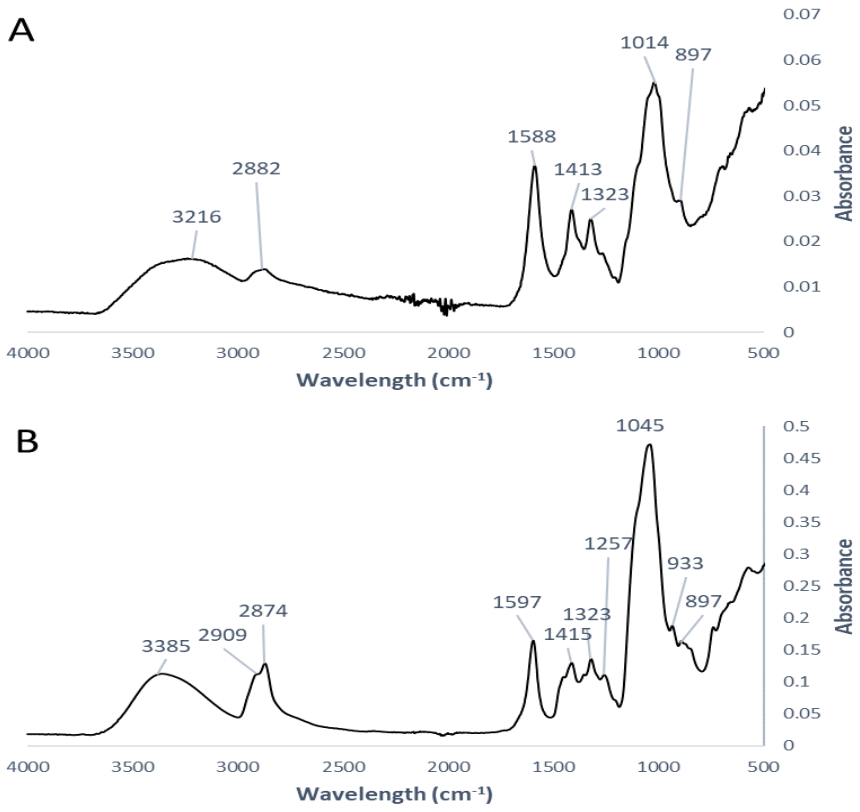

Figure 4.2: FTIR spectra of A) native CMC and B) CMC crosslinked with EGDE.

CMC is made up of a glucose ring with one or more carboxymethyl side groups (depending on the degree of substitution). As a result, the major FTIR characteristic peaks of CMC are the O–H stretch, C–H stretch, –COO stretch from the carboxyl group, C–H bend, C–O stretch of the glycosidic bond, C–C bend. These vibrations can be assigned to the respective peaks at 3240 cm^{-1}, 2910 cm^{-1} and 2880 cm^{-1},

1588 cm^{-1}, 1414 cm^{-1}, 1320 cm^{-1}, 1094 cm^{-1}, and 1020 cm^{-1}. Due to the close proximity of the C–O stretch and C–C bending, the broader peak at 1020 cm^{-1} is collectively considered as the merger of the two vibrations. It is worth noting that the peak around 1410 cm^{-1} has been reported in the literature as originating from different functional groups. Some assign the peak to be an asymmetric stretch of the carboxyl group as salts [29], others assign the peak to be CH bending [28, 38].

The FTIR spectrum of EGDE crosslinked CMC is not expected to show any new peaks when compared to naive CMC, since the new chemical bonds introduced from the crosslinking are similar to the ones already present in native CMC. However, some small peak shifts and changes in peak appearance will be noticeable if crosslinking has occurred, due to changed chemical structure and addition of EGDE. In both of the spectra, there is a weak peak around 1250 cm^{-1} present. In the crosslinked spectrum we can also see three weak peaks around 930 cm^{-1}, 840 cm^{-1}. These two peaks along with the 1250 cm^{-1} peak are associated with epoxide group of the EGDE [39], which suggests that there could still be some unreacted EGDE left in the aerogel. Further, this could indicate that the gels should be washed for longer to fully remove all the unreacted species. Peaks between 880 and 840 cm^{-1} peaks have been associated with C–H deformation of the glucose ring [28]; however, the C–H deformation most likely belongs to the peak at 986 cm^{-1} as it also can be seen in the native CMC.

4.4 Morphology of Aerogels and Impregnated Aerogels

The morphology of aerogels and impregnated aerogels were investigated using SEM. The following aerogels were analyzed:

- Aerogel frozen at -18 °C
- Aerogel frozen at -196 °C
- Aerogel frozen at -18 °C, injected with LNP solution (dry state)
- Aerogel frozen at -196 °C, injected with LNP solution (dry state)
- Aerogel frozen at -196 °C, injected with LNP solution (wet state)

The SEM images of the aerogel samples can be seen in Figure 4.3. It can be seen (Figures 4.3A and 4.3C) that freezing the gel at -18 °C results in a large smooth surface and larger pores with relatively thin walls. Decreasing the freezing temperature to - 196 °C (Figures 4.3B, 4.3D, and 4.3E) results in gels with areas of large smooth surfaces and areas with many smaller pores.

In Figure 4.3C, there are considerable amounts of micro-holes and micro-craters. This can also be seen in Figure B.2 and B.3, but to a lesser extent. It is possible that these holes and craters are formed during injection of LNP solution as well as during freezing at -18 °C. The size of the holes and crates are between 2 μm and 100 nm. As it seems like both freezing the hydrogel at high temperatures and injecting the aerogel in a dry state with LNPs causes these holes and craters to form, it could

explain why the aerogel in Figure 4.3C has such a considerable amount of them. The holes could be from air bubbles entrapped in the CMC walls (introduced either from the synthesis or from injection) that have escaped during freeze-drying. However, it may also be caused by interactions with LNPs have opened very thin parts of the walls.

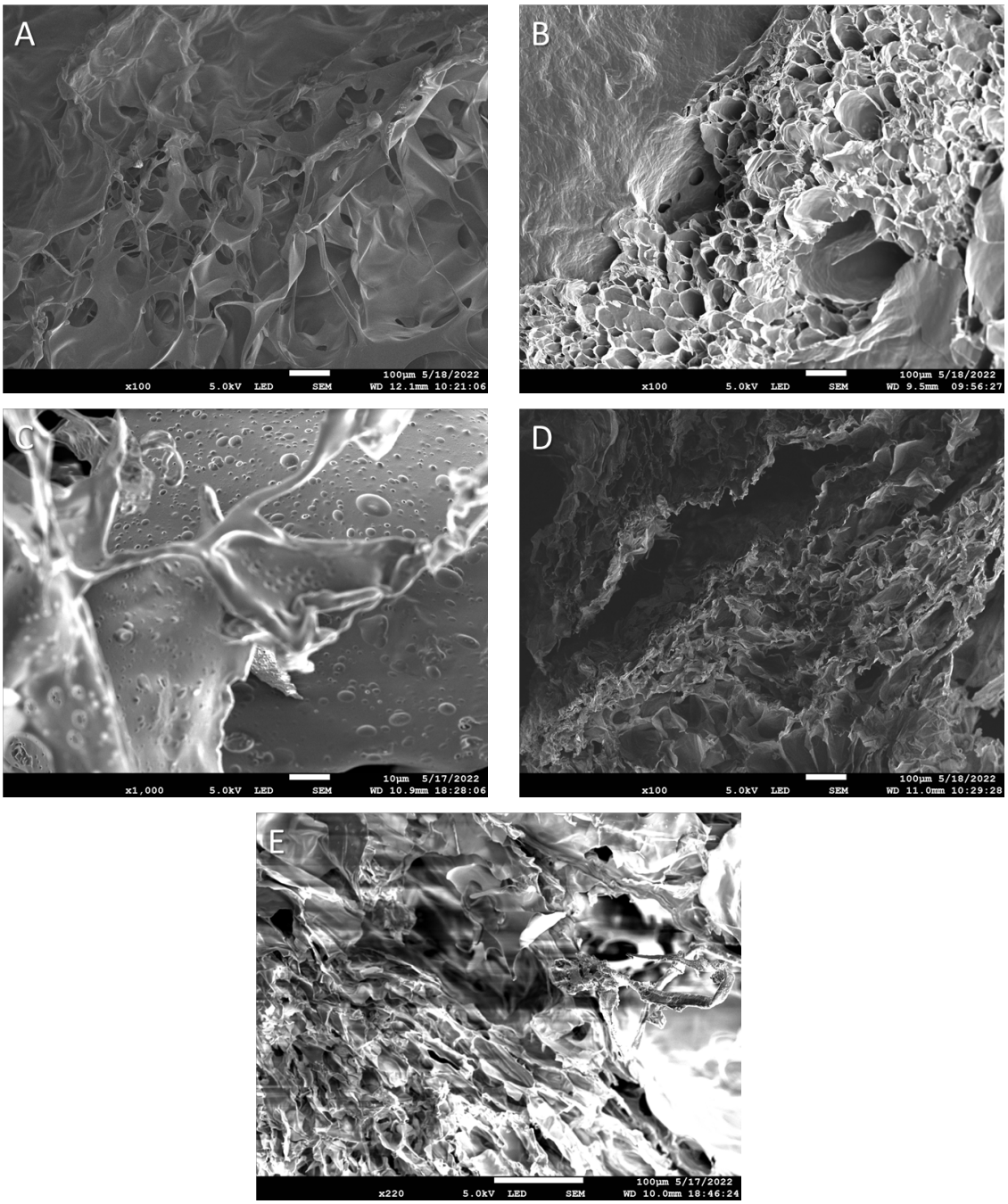

Figure 4.3: SEM image of the frozen aerogels. A) frozen at -18 °C, B) frozen at -196 °C, C) injected in dry state with LNPs and frozen at -18 °C, D) injected in wet state with LNPs and frozen at -196 °C, and E) injected in dry state with LNPs and frozen at -196 °C. All aerogels have the same EGDE and CMC concentration as well as synthesis conditions.

In Figure B.1, there is a lot of small debris in the aerogel frozen at -196 °C. This is most likely due to how the sample was cut and handled; however, it could also be debris from cracking of the pore walls during freeze-drying due to a combination of weak pore walls and strong capillary forces of water.

4.5 Preparation of LNPs

The LNPs synthesized via an anti-solvent method were analyzed with SEM. From the SEM images, it was determined that the average particle size for the unloaded LNPs was around 71.6 nm, while naproxen-loaded LNPs had an average particle size of around 81 nm. As can be seen in Figure 4.4 there is quite a large variance in size. The smallest particles were 31.5 nm for unloaded LNPs and 26.5 nm for naproxen-loaded LNPs, while the largest particles were 127 nm and 140 nm, respectively. The size increase has been observed in other studies [10, 33] when drug-loading LNPs. This is due to the added molecules being entrapped in the LNPs during the nanoparticle formation. This can be used as an indication of how good the drug is to load using entrapment as the loading method. The better the drug is at being entrapped (*i.e.* smaller and more hydrophobic), the more optimal the entrapping is and a smaller average particle size should be observed [33].

From Figure 4.4, it is evident that the formed nanoparticles have a spherical shape, regardless of if the LNPs were drug-loaded or not. However, the naproxen-loaded LNPs (Figure 4.4B) have some elongated particles present.

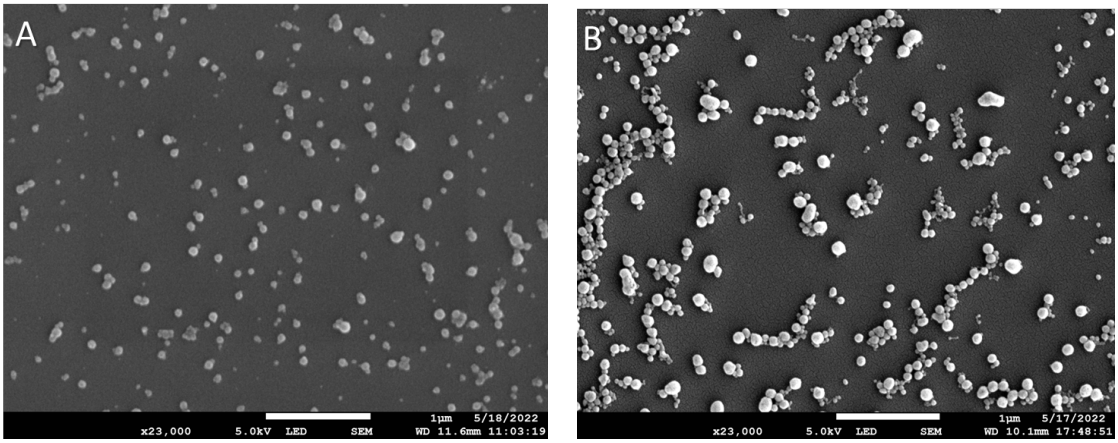

Figure 4.4: SEM images of LNPs A) unloaded, and B) naproxen-loaded.

4.6 Loading Capacity and Encapsulation Efficiency

From the absorption data obtained from the UV-Vis measurements, the loading capacity and encapsulation efficiency were calculated (see Table 4.2). The loading capacity was calculated to be 10.3%, which was in expected. The encapsulation

efficiency was calculated to be 47.6%, which was much lower than expected. The yield was 47.4% which was much lower than expected.

Table 4.2: The calculated values of loading capacity, encapsulation efficiency, and yield for naproxen-loaded LNPs.

Loading Capacity (%)	Encapsulation Efficiency (%)	Yield (%)
10.3	47.6	47.4

As was mentioned in Section 2.7, LNPs have a low loading capacity but a high encapsulation efficiency for hydrophobic drugs. Such a low loading capacity is expected for LNPs; however, the low encapsulation efficiency is not expected. Although naproxen is considered practically water-insoluble (solubility of 15.9 mg/L [40] in water at 25 °C), it is much more water-soluble than the other drugs used by Alqahtani *et al.* and Figueiredo *et al.*. This could be an explanation for the low encapsulation efficiency; however, Li *et al.* used ibuprofen, which is more water-soluble than naproxen, and achieved an encapsulation efficiency of 74%. This suggests that modification of the LNPs or lignin is needed to increase the encapsulation efficiency and loading capacity. The drug-loading method may also influence the encapsulation efficiency and loading capacity, making it possible that other methods are more effective than entrapment.

4.7 Impregnation of Aerogel and Hydrogel with LNPs

Two different ways of impregnating hydrogels and aerogels were tested: injection and immersion. The immersed hydrogel and aerogels were after 3 days only brown on the outside and white on the inside (see Figure A.5 and A.6. This indicates that the LNPs did not penetrate deeply into the gels via diffusion. Longer diffusion times may be required for deeper penetration; nonetheless, this would be even more time-consuming, especially if the size of the aerogel is scaled-up.

In injection, on the other hand, LNPs can penetrate more deeply but the results of injecting hydrogels and aerogels were quite different. When injecting hydrogels with LNPs, the solution would only spread along "channels" and created a more network-like spreading than a homogeneous one (see Figure A.9). Small pockets of LNP solution would be created around the needle tip during injection, but they would burst if too much solution was introduced at the same spot. Although the injected hydrogels were left for 24 h to allow the LNP solution to diffuse, no apparent changes were noticed after 3 days. Injection of LNP solution into aerogels resulted in a more homogeneous color spread (see Figure A.7). As it can be seen, the cross-section of injected aerogels is fully brown, indicating that the LNP solution has fully penetrated the aerogels.

From the morphological studies of the impregnated aerogels, no LNPs were observed. For the injected hydrogel, it is most likely that the LNPs are only present in

the "channels" created during injection; thus, making it difficult to find any LNPs elsewhere. It is also unclear if LNPs are not present in the injected aerogel, either because the sample did not have any on the surface of the sample or it could be that the LNPs have dissolved due to too high pH in the gel. The LNP solution was allowed to diffuse for 3 days, which could result in the LNPs starting to dissolve if the gel had a too high pH. Nonetheless, it is inconclusive if LNPs actually were present or not.

5

Conclusion

The aim of this project was to create a wound dressing impregnated with a pH-responsive drug-loaded LNPs that can be used for chronic wounds.

The wound dressing was prepared by first producing an EGDE cross-linked CMC aerogel and freeze-drying it. Different synthesis conditions were investigated to better understand and optimize the aerogel. Increasing CMC and EGDE concentrations resulted in more stable aerogels that could withstand compression even after swelling. Using CMC with high molecular weight resulted in less CMC being possible to dissolve and required higher EGDE concentrations to make a stable aerogel, compared to a lower molecular weight CMC. Decreasing the NaOH concentration during synthesis resulted in aerogels with higher swelling capacity; however, decreasing the NaOH concentration below 0.1 M resulted in no gel formation. Using lower molecular weight CMC grades, a stable aerogel can be formed with lower concentrations of EGDE, and the resulting aerogel have a high swelling capacity.

Drug-loading LNPs with naproxen via an anti-solvent precipitation method was shown to be possible. The loading capacity was low and the encapsulation efficiency was also quite low, which was unexpected. The synthesized LNPs, drug-loaded and unloaded, were quite small in diameter and the size distribution was large. The produced LNPs were in general spherical, especially for unloaded LNPs, but some elongated particles were formed when loading the LNPs with drugs.

Impregnating the aerogels and hydrogels with LNPs was possible, however, the effect varied depending on the method used and the type of gel. Hydrogels were overall more difficult to impregnate via immersion and injection compared to aerogels. When immersed the lignin did not diffuse deeply into the gel and was only seen around the edges. Injection resulted in deeper penetration but did not spread homogeneously and only spread in specific network-like channels. Aerogels immersed in LNP solution showed similar results to immersed hydrogels. Aerogels injected with LNP solution showed a much more homogeneous spread. Nonetheless, no LNPs were observed in SEM in either of the LNP impregnated gels.

5.1 Future Work

Moving forward, it is important to investigate if the LNPs are actually present in the aerogel after impregnation and do a release study to see how controlled the drug release is and if it is pH-responsive. Furthermore, it should be investigated if antibiotics can be loaded and study the drug release as well as loading capacity and encapsulation efficiency.

It is also of interest to either further optimize the aerogel synthesis or try other routes to synthesize aerogels. Due to LNPs not having high stability at alkaline pH a more accurate way to measure the gel's pH should be investigated—if EGDE will be used as a cross-linker. Cryogelation (i.e. forming the gel under cryogenic conditions) is an alternative route where the same chemicals can be used to form the hydrogel. It has the advantage of requiring lower concentrations of cross-linker since the cross-linker and CMC becomes concentrated in specific areas due to the formation of ice crystals. The downside is the longer gelation time. Another route would be using a cross-linker that forms a gel under acidic conditions such as citric acid. It has the advantage of not requiring long washing times as the LNPs are stable in acidic pH.

Due to injection and immersion not being optimal ways to impregnate aerogels or hydrogels, it should be investigated if the LNPs can be added before the gel has formed. Either the thermal stability of LNPs should be investigated due to most cross-linkers requiring high temperatures or producing a physically cross-linked gel or utilizing cryogelation with a cross-linker in acidic conditions.

Bibliography

[1] Ruilong Zhao, Helena Liang, Elizabeth Clarke, Christopher Jackson, and Meilang Xue. "Inflammation in chronic wounds". In: *International journal of molecular sciences* 17.12 (2016), p. 2085. DOI: https://doi.org/10.3390/ijms17122085.

[2] Robert G. Frykberg and Jaminelli Banks. "Challenges in the Treatment of Chronic Wounds". In: *Advances in Wound Care* 4.9 (2015), pp. 560–582. DOI: https://doi.org/10.1089/wound.2015.0635.

[3] Elof Eriksson, Paul Y. Liu, Gregory S. Schultz, Manuela M. Martins-Green, Rica Tanaka, Dot Weir, Lisa J. Gould, David G. Armstrong, Gary W. Gibbons, Randy Wolcott, Oluyinka O. Olutoye, Robert S. Kirsner, and Geoffrey C. Gurtner. "Chronic wounds: Treatment consensus". In: *Wound Repair and Regeneration* 30.2 (2022), pp. 156–171. DOI: https://doi.org/10.1111/wrr.12994.

[4] Joshua S. Boateng, Kerr H. Matthews, Howard N.E. Stevens, and Gillian M. Eccleston. "Wound Healing Dressings and Drug Delivery Systems: A Review". In: *Journal of Pharmaceutical Sciences* 97.8 (2008), pp. 2892–2923. DOI: https://doi.org/10.1002/jps.21210.

[5] Daniel G. Metcalf, Marieke Haalboom, Philip G. Bowler, Clemens Gamerith, Eva Sigl, Andrea Heinzle, and Michael W.M. Burnet. "Elevated wound fluid pH correlates with increased risk of wound infection". In: *Wound Medicine* 26.1 (2019), p. 100166. DOI: https://doi.org/10.1016/j.wndm.2019.100166.

[6] Saghi Saghazadeh, Chiara Rinoldi, Maik Schot, Sara Saheb Kashaf, Fatemeh Sharifi, Elmira Jalilian, Kristo Nuutila, Giorgio Giatsidis, Pooria Mostafalu, Hossein Derakhshandeh, Kan Yue, Wojciech Swieszkowski, Adnan Memic, Ali Tamayol, and Ali Khademhosseini. "Drug delivery systems and materials for wound healing applications". In: *Advanced Drug Delivery Reviews* 127 (2018). Skin-Associated Drug Delivery, pp. 138–166. DOI: https://doi.org/10.1016/j.addr.2018.04.008.

[7] Erfan Rezvani Ghomi, Shahla Khalili, Saied Nouri Khorasani, Rasoul Esmaeely Neisiany, and Seeram Ramakrishna. "Wound dressings: Current advances and future directions". In: *Journal of Applied Polymer Science* 136.27 (2019), p. 47738. DOI: https://doi.org/10.1002/app.47738.

[8] Ruth Ellen Jones, Deshka S. Foster, and Michael T. Longaker. "Management of Chronic Wounds—2018". In: *JAMA* 320.14 (Oct. 2018), pp. 1481–1482. DOI: https://doi.org/10.1001/jama.2018.12426.

[9] Vimala Kanikireddy, Kokkarachedu Varaprasad, Tippabattini Jayaramudu, Chandrasekaran Karthikeyan, and Rotimi Sadiku. "Carboxymethyl cellulose-

based materials for infection control and wound healing: A review". In: *International Journal of Biological Macromolecules* 164 (2020), pp. 963–975. DOI: https://doi.org/10.1016/j.ijbiomac.2020.07.160.

[10] Mohammed S Alqahtani, Ali Alqahtani, Abdullah Al-Thabit, Monzurul Roni, and Rabbani Syed. "Novel lignin nanoparticles for oral drug delivery". In: *Journal of Materials Chemistry B* 7.28 (2019), pp. 4461–4473. DOI: https://doi.org/10.1039/C9TB00594C.

[11] Christian J Wijaya, Suryadi Ismadji, and Setiyo Gunawan. "A review of lignocellulosic-derived nanoparticles for drug delivery applications: lignin nanoparticles, xylan nanoparticles, and cellulose nanocrystals". In: *Molecules* 26.3 (2021), p. 676. DOI: https://doi.org/10.3390/molecules26030676.

[12] Muhammad Maaz Arif, Shahzad Maqsood Khan, Nafisa Gull, Tanveer A. Tabish, Saba Zia, Rafi Ullah Khan, Sayed Muhammad Awais, and Muhammad Arif Butt. "Polymer-based biomaterials for chronic wound management: Promises and challenges". In: *International Journal of Pharmaceutics* 598 (2021), pp. 1218–1234. DOI: https://doi.org/10.1016/j.ijpharm.2021.120270.

[13] Kathryn Vowden and Peter Vowden. "Wound dressings: principles and practice". In: *Surgery (Oxford)* 35.9 (2017), pp. 489–494. DOI: https://doi.org/10.1016/j.mpsur.2017.06.005.

[14] Yimin Qin. "Advanced wound dressings". In: *Journal of the Textile Institute* 92.2 (2001), pp. 127–138. DOI: https://doi.org/10.1080/00405000108659563.

[15] Dong Liu, Fang Yang, Fei Xiong, and Ning Gu. "The smart drug delivery system and its clinical potential". In: *Theranostics* 6.9 (2016), p. 1306. DOI: https://doi.org/10.7150/thno.14858.

[16] Yao Fu and Weiyuan John Kao. "Drug release kinetics and transport mechanisms of non-degradable and degradable polymeric delivery systems". In: *Expert Opinion on Drug Delivery* 7.4 (2010), pp. 429–444. DOI: 10.1517/17425241003602259.

[17] Rajesh Singh and James W Lillard Jr. "Nanoparticle-based targeted drug delivery". In: *Experimental and molecular pathology* 86.3 (2009), pp. 215–223. DOI: https://doi.org/10.1016/j.yexmp.2008.12.004.

[18] Lin-Yu Long, Yun-Xuan Weng, and Yu-Zhong Wang. "Cellulose Aerogels: Synthesis, Applications, and Prospects". In: *Polymers* 10.6 (2018). DOI: https://doi.org/10.3390/polym10060623.

[19] J. V. Alemán, A. V. Chadwick, J. He, M. Hess, K. Horie, R. G. Jones, P. Kratochvíl, I. Meisel, I. Mita, G. Moad, S. Penczek, and R. F. T. Stepto. "Definitions of terms relating to the structure and processing of sols, gels, networks, and inorganic-organic hybrid materials (IUPAC Recommendations 2007)". In: *Pure and Applied Chemistry* 79.10 (2007), pp. 1801–1829. DOI: https://doi.org/10.1351/pac200779101801.

[20] Mehrez E. El-Naggar, Sarah I. Othman, Ahmed A. Allam, and Osama M. Morsy. "Synthesis, drying process and medical application of polysaccharide-based aerogels". In: *International Journal of Biological Macromolecules* 145 (2020), pp. 1115–1128. DOI: https://doi.org/10.1016/j.ijbiomac.2019.10.037.

[21] Mariangela Guastaferro, Ernesto Reverchon, and Lucia Baldino. "Polysaccharide-Based Aerogel Production for Biomedical Applications: A Comparative Review". In: *Materials* 14.7 (2021). DOI: https://doi.org/10.3390/ma14071631.

[22] Xiaoping Shen, Julia L. Shamshina, Paula Berton, Gabriela Gurau, and Robin D. Rogers. "Hydrogels based on cellulose and chitin: fabrication, properties, and applications". In: *Green Chem.* 18 (1 2016), pp. 53–75. DOI: https://doi.org/10.1039/C5GC02396C.

[23] Dimitri Eigel, Carsten Werner, and Ben Newland. "Cryogel biomaterials for neuroscience applications". In: *Neurochemistry International* 147 (2021), p. 105012. DOI: https://doi.org/10.1016/j.neuint.2021.105012.

[24] Irina V. Tyshkunova, Daria N. Poshina, and Yury A. Skorik. "Cellulose Cryogels as Promising Materials for Biomedical Applications". In: *International Journal of Molecular Sciences* 23.4 (2022). DOI: https://doi.org/10.3390/ijms23042037.

[25] Anna Ström, Anette Larsson, and Oguz Okay. "Preparation and physical properties of hyaluronic acid-based cryogels". In: *Journal of Applied Polymer Science* 132.29 (2015). DOI: https://doi.org/10.1002/app.42194.

[26] J. Berger, M. Reist, J.M. Mayer, O. Felt, N.A. Peppas, and R. Gurny. "Structure and interactions in covalently and ionically crosslinked chitosan hydrogels for biomedical applications". In: *European Journal of Pharmaceutics and Biopharmaceutics* 57.1 (2004), pp. 19–34. DOI: https://doi.org/10.1016/S0939-6411(03)00161-9.

[27] Qinfeng He, Ryosuke Kusumi, Satoshi Kimura, Ung-Jin Kim, Kenzo Deguchi, Shinobu Ohki, Atsushi Goto, Tadashi Shimizu, and Masahisa Wada. "Highly swellable hydrogel of regioselectively aminated (1→3)-α-d-glucan crosslinked with ethylene glycol diglycidyl ether". In: *Carbohydrate Polymers* 237 (2020), p. 116189. DOI: https://doi.org/10.1016/j.carbpol.2020.116189.

[28] Debashis Kundu and Tamal Banerjee. "Carboxymethyl Cellulose–Xylan Hydrogel: Synthesis, Characterization, and in Vitro Release of Vitamin B12". In: *ACS Omega* 4.3 (2019), pp. 4793–4803. DOI: https://doi.org/10.1021/acsomega.8b03671.

[29] Daham Jeong, Chulgu Kim, Yohan Kim, and Seunho Jung. "Dual crosslinked carboxymethyl cellulose/polyacrylamide interpenetrating hydrogels with highly enhanced mechanical strength and superabsorbent properties". In: *European Polymer Journal* 127 (2020), p. 109586. DOI: https://doi.org/10.1016/j.eurpolymj.2020.109586.

[30] Dong Tian, Jinguang Hu, Richard P. Chandra, Jack N. Saddler, and Canhui Lu. "Valorizing Recalcitrant Cellulolytic Enzyme Lignin via Lignin Nanoparticles Fabrication in an Integrated Biorefinery". In: *ACS Sustainable Chemistry & Engineering* 5.3 (2017), pp. 2702–2710. DOI: https://doi.org/10.1021/acssuschemeng.6b03043.

[31] Willian Daniel Hahn Schneider, Aldo José Pinheiro Dillon, and Marli Camassola. "Lignin nanoparticles enter the scene: A promising versatile green tool for multiple applications". In: *Biotechnology Advances* 47 (2021), p. 107685. DOI: https://doi.org/10.1016/j.biotechadv.2020.107685.

[32] Mika Henrikki Sipponen, Heiko Lange, Claudia Crestini, Alexander Henn, and Monika Österberg. "Lignin for Nano- and Microscaled Carrier Systems: Applications, Trends, and Challenges". In: *ChemSusChem* 12.10 (2019), pp. 2039–2054. DOI: https://doi.org/10.1002/cssc.201900480.

[33] Patrícia Figueiredo, Kalle Lintinen, Alexandros Kiriazis, Ville Hynninen, Zehua Liu, Tomás Bauleth-Ramos, Antti Rahikkala, Alexandra Correia, Tomáš Kohout, Bruno Sarmento, Jari Yli-Kauhaluoma, Jouni Hirvonen, Olli Ikkala, Mauri A. Kostiainen, and Hélder A. Santos. "In vitro evaluation of biodegradable lignin-based nanoparticles for drug delivery and enhanced antiproliferation effect in cancer cells". In: *Biomaterials* 121 (2017), pp. 97–108. DOI: https://doi.org/10.1016/j.biomaterials.2016.12.034.

[34] Yuanyuan Li, Xueqing Qiu, Yong Qian, Wenlong Xiong, and Dongjie Yang. "pH-responsive lignin-based complex micelles: Preparation, characterization and application in oral drug delivery". In: *Chemical Engineering Journal* 327 (2017), pp. 1176–1183. DOI: https://doi.org/10.1016/j.cej.2017.07.022.

[35] M. Hazwan Hussin, Jimmy Nelson Appaturi, Ng Eng Poh, Nur Hanis Abd Latif, Nicolas Brosse, Isabelle Ziegler-Devin, Henri Vahabi, Firda Aulya Syamani, Widya Fatriasari, Nissa Nurfajrin Solihat, Azizatul Karimah, Apri Heri Iswanto, Siti Hajar Sekeri, and Mohamad Nasir Mohamad Ibrahim. "A recent advancement on preparation, characterization and application of nanolignin". In: *International Journal of Biological Macromolecules* 200 (2022), pp. 303–326. DOI: https://doi.org/10.1016/j.ijbiomac.2022.01.007.

[36] Yun Liu, Guangze Yang, Song Jin, Letao Xu, and Chun-Xia Zhao. "Development of High-Drug-Loading Nanoparticles". In: *ChemPlusChem* 85.9 (2020), pp. 2143–2157. DOI: https://doi.org/10.1002/cplu.202000496.

[37] Yiming Chen, Lin Zhang, Yang Yang, Bo Pang, Wenhui Xu, Gaigai Duan, Shaohua Jiang, and Kai Zhang. "Recent Progress on Nanocellulose Aerogels: Preparation, Modification, Composite Fabrication, Applications". In: *Advanced Materials* 33.11 (2021), p. 2005569. DOI: https://doi.org/10.1002/adma.202005569.

[38] Hiroyuki Kono. "Characterization and properties of carboxymethyl cellulose hydrogels crosslinked by polyethylene glycol". In: *Carbohydrate Polymers* 106 (2014), pp. 84–93. DOI: https://doi.org/10.1016/j.carbpol.2014.02.020.

[39] Donal Pavia, Gary Lampman, George Kriz, and James Vyvyan. *Introduction to spectroscopy/ Donald L. Pavia, Gary M. Lampman, George S. Kriz, and James R. Vyvyan.* Aug. 2015. ISBN: 978-1-285-46012-3.

[40] SH Yalkowsky and Y He. "An extensive compilation of aqueous solubility data for organic compounds extracted from the AQUASOL database". In: *Handbook of Aqueous Solubility Data* (2003), p. 377. DOI: https://doi.org/10.1201/EBK1439802458.

A

Appendix 1

Figure A.1: Freeze-dried aerogel with needle-like surface holes.

Figure A.2: Freeze-dried aerogel (9 wt.% EGDE, 2.2 wt.% CMC, 0.1 M NaOH) with surface holes

Figure A.3: Surface of aerogel frozen at -196 °C after freeze-drying with a cracked surface.

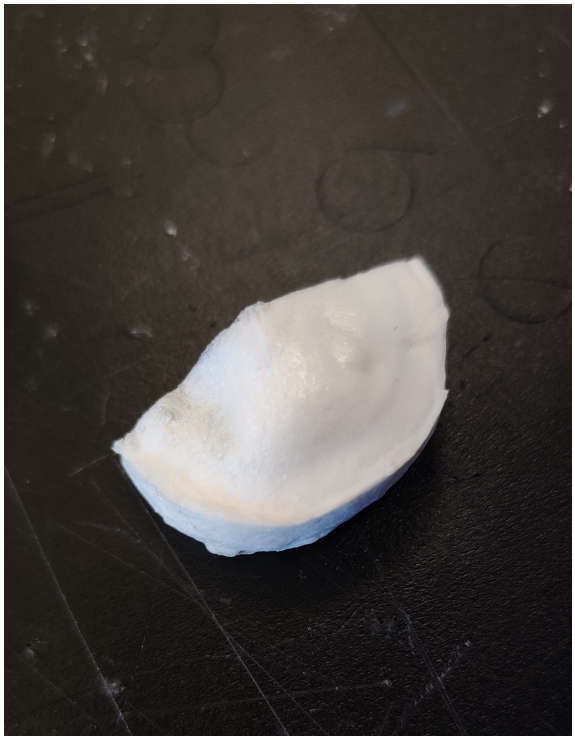

Figure A.4: Surface of aerogel frozen at -196 °C after freeze-drying with a non-cracked surface.

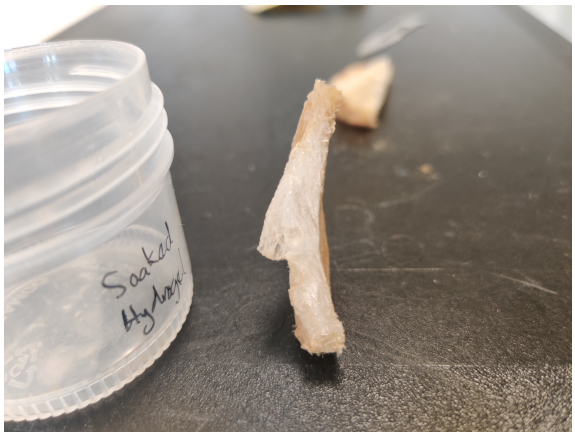

Figure A.5: Aerogel that have been immersed in LNP solution in a wet state and then freeze-dried.

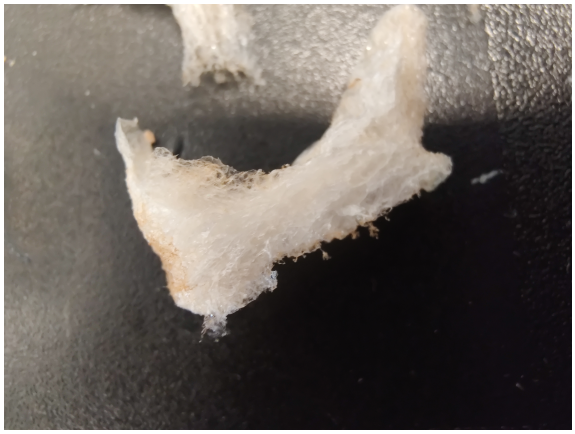

Figure A.6: Aerogel that have been immersed in LNP solution in a dry state and then freeze-dried.

Figure A.7: Aerogel that have been injected with LNP solution in a dry state and then freeze-dried.

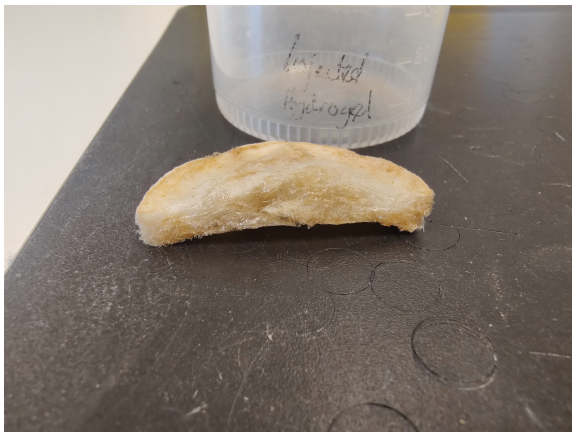

Figure A.8: Aerogel that have been injected with LNP solution in a wet state and then freeze-dried.

Figure A.9: Hydrogel that have been injected with LNP solution that shows the spreading behavior of the LNP solution.

B

Appendix 2

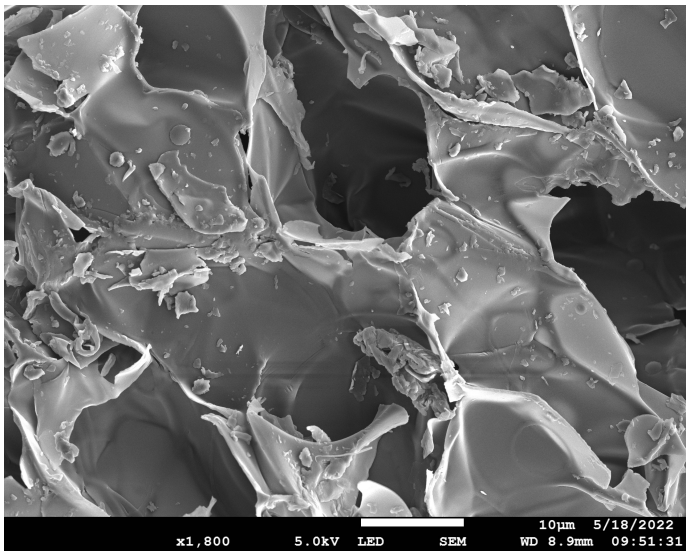

Figure B.1: SEM image of an aerogel frozen at -196 °C.

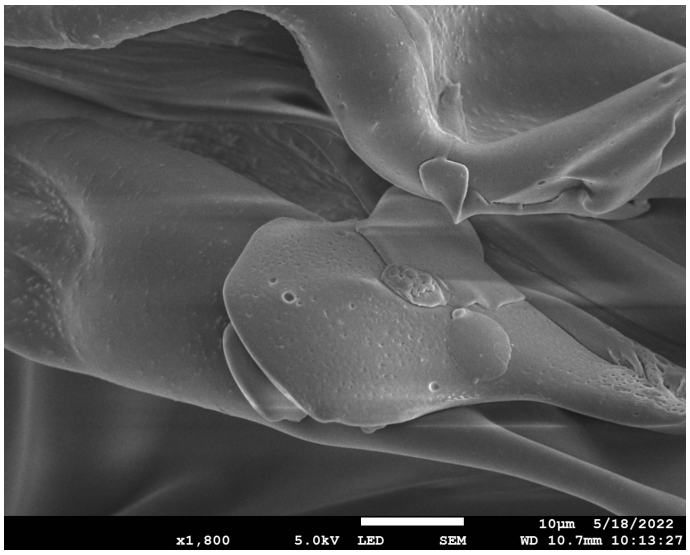

Figure B.2: SEM image of an aerogel frozen at -18 °C.

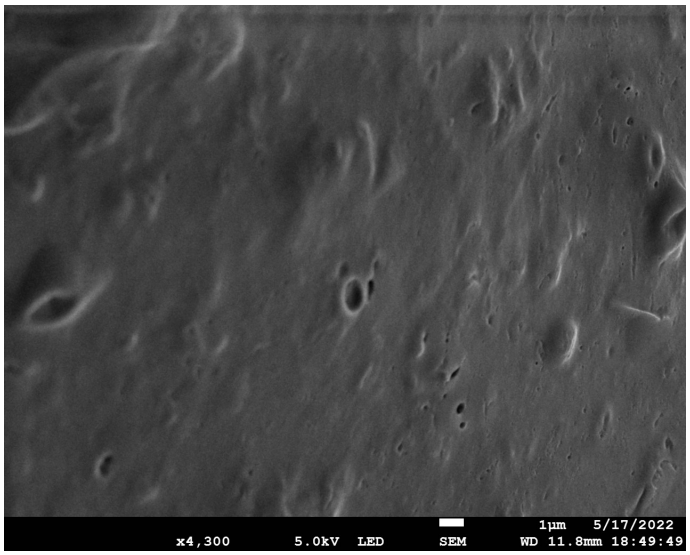

Figure B.3: SEM image of an aerogel frozen at -196 °C. and injected with LNP solution.

C

Appendix 3

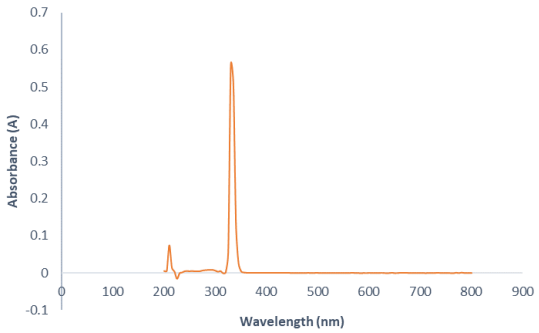

Figure C.1: UV-Vis curve of Naproxen (0.0075 mg/mL) in 50 V/V% water and acetone. The 330 nm peak belongs to Naproxen.

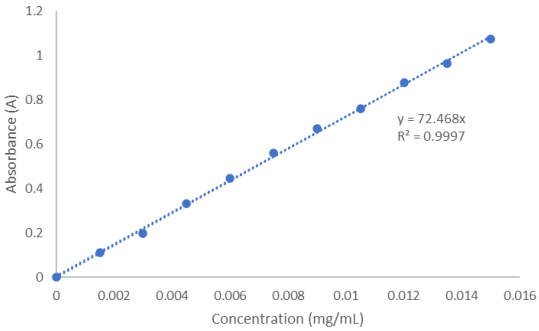

Figure C.2: Standard curve of Naproxen in 50 V/V% water and acetone.

DEPARTMENT OF SOME SUBJECT OR TECHNOLOGY
CHALMERS UNIVERSITY OF TECHNOLOGY
Gothenburg, Sweden
www.chalmers.se

CHALMERS
UNIVERSITY OF TECHNOLOGY